

Supporting Information

Series of Dysprosium Clusters Assembled by a Substitution Effect-Driven Out-to-In Growth Mechanism

Hai-Ling Wang,^a Tong Liu,^a Zhong-Hong Zhu,^{a,b,*} Jin-Mei Peng,^a Hua-Hong Zou,^{a,*} Fu-Pei Liang^{a,c,*}

^aState Key Laboratory for Chemistry and Molecular Engineering of Medicinal Resources, School of Chemistry and Pharmacy of Guangxi Normal University, Guilin 541004, P. R. China

^bState Key Laboratory of Luminescent Materials and Devices, School of Materials Science and Engineering, South China University of Technology, 510640 Guangzhou, China

^cGuangxi Key Laboratory of Electrochemical and Magnetochemical Functional Materials, College of Chemistry and Bioengineering, Guilin University of Technology, Guilin 541004, P. R. China

*E-mail (Corresponding author): 18317725515@163.com (Z.-H. Zhu), gxnuchem@foxmail.com (H.-H. Zou), fliangoffice@yahoo.com (F.-P. Liang).

Table of Contents:

Supporting Tables	
Table S1	Crystallographic data of the clusters 1–3 .
Table S2	Selected bond lengths (\AA) and angles ($^\circ$) of 1 .
Table S3	Selected bond lengths (\AA) and angles ($^\circ$) of 2 .
Table S4	Selected bond lengths (\AA) and angles ($^\circ$) of 3 .
Supporting Figures	
Figure S1	Infrared spectra (IR) of clusters 1–3 .
Figure S2	TG curve of clusters 1–3 .
Figure S3	Powder diffraction pattern (PXRD) of clusters 1–3 .
Figure S4	Temperature dependence of $\chi_m T$ for clusters 1–3 (a, c and e); M vs. H plots of clusters 1–3 (b, d and f).
Figure S5	Loop curve graph of clusters 1–3 at 2 K.
Figure S6	The imaginary parts of the AC susceptibility of clusters 1–3 tested under external DC field values in the range of 0-4000 Oe at 2 K for 1 (left), 2 (middle), and 3 (right).
Figure S7	$\ln(\tau)$ vs. T^{-1} plots for 1 (a), 2 (b), and 3 (c), the solid lines show the best fits with the Debye formula (linear).

Experimental Section

Materials and Measurements.

All reagents were obtained from commercial sources and used without further purification. Elemental analyses for C, and H were performed on a vario MICRO cube. Infrared spectra were recorded by transmission through KBr pellets containing *ca.* 0.5% of the complexes using a PE Spectrum FT-IR spectrometer (400-4,000 cm⁻¹; Figure S1). Thermogravimetric analyses (TGA) were conducted in a flow of nitrogen at a heating rate of 5 °C/min using a NETZSCH TG 209 F3 (Figure S2). Powder X-ray diffraction (PXRD) spectra were recorded on either a D8 Advance (Bruker) diffractometer at 293 K (Mo-K α). The samples were prepared by crushing crystals and the powder placed on a grooved aluminum plate. Diffraction patterns were recorded from 5° to 55° at a rate of 5° min⁻¹ (Figure S3). Measurements of magnetic susceptibility were carried out within the temperature range of 2–300 K using a Quantum Design MPMS SQUID magnetometer equipped with a 7 T magnet. The diamagnetic corrections for these complexes were estimated using Pascal's constants, and magnetic data were corrected for diamagnetic contributions of the sample holder. Alternating current susceptibility measurements were performed from powdered samples to determine the in-phase and out-of-phase components of the magnetic susceptibility. The data were collected by increasing the temperature from 2 K to 15 K within frequencies ranging from 1 to 1,000 Hz, under 0 Oe and 1200 Oe. In the samples where free movement of crystallites was prevented, silicone grease was employed for embedding.

Single-crystal X-ray crystallography.

Diffraction data for the complex were collected on a Bruker SMART CCD diffractometer (Mo-K α radiation and $\lambda = 0.71073 \text{ \AA}$) in Φ and ω scan modes. The structures were solved by direct methods, followed by difference Fourier syntheses, and then refined by full-matrix least-squares techniques on F^2 using *SHELXL*^[1]. All other non-hydrogen atoms were refined with anisotropic thermal parameters. Hydrogen atoms were placed at calculated positions and isotropically refined using a riding model. Table S3 summarizes X-ray crystallographic data and refinement details for the complex. The CCDC reference numbers are 2058342, 2058346 and 2058348 for **1–3**.

[1]Sheldrick, G. M. *Acta Crystallogr., Sect. C: Struct. Chem.* **2015**, *71*, 3-8.

The synthesis method.

H₄L¹–H₄L³: The synthesis of organic ligands H₄L¹–H₄L³ refers to the reported method.^[2]

1: Add 0.05 mmol (approximately 25 mg) ligand H₄L¹, 0.4 mmol Dy(NO₃)₃·6H₂O (approximately 183 mg), 1.5 mL CH₃OH, 0.5 mL CH₃CN, and 0.15 mL triethylamine to the Pyrex whose one end is about 25 cm long In the tube, shake and sonicate for 15 min. Place the sealed Pyrex tube in an oven at 80 °C, take it out three days later, slowly cool to room temperature, and precipitate yellow lumpy crystals. The yield is about 52.3% (calculated with the amount of ligand). Elemental analysis theoretical value (C₈₄H₉₃Dy₁₆N₂₉O₈₀): C, 18.72%; H, 1.74%; N, 7.54%; experimental value: C, 18.44%; H, 1.95%; N, 7.23%. Infrared spectrum data (IR, KBr pellet, cm⁻¹): 3343.17(s), 1614.29(m), 1501.04(w), 1461.39(w), 1384.32(vs), 1201.61(w), 866.95(w), 760.12(w)).

2: Add 0.05 mmol (approximately 27 mg) ligand H₄L², 0.4 mmol Dy(NO₃)₃·6H₂O (approximately 183 mg), 1.5 mL CH₃OH, 0.5 mL CH₃CN, and 0.15 mL triethylamine to the Pyrex whose one end is about 25 cm long In the tube, shake and sonicate for 15 min. Place the sealed Pyrex tube in an oven at 80 °C, take it out three days later, slowly cool to room temperature, and precipitate brown lumpy

crystals. The yield is about 55.4% (calculated with the amount of ligand). Elemental analysis theoretical value ($C_{127}H_{134}Dy_{10}N_{30}O_{53}$): C, 33.50%; H, 2.97%; N, 9.23%; experimental value: C, 33.22%; H, 3.12%; N, 9.11%. Infrared spectrum data (IR, KBr pellet, cm^{-1}): 3470.78(s), 2376.35(w), 1606.06(vs), 1501.31(s), 1430.00(s), 1384.37(m), 1221.08(m), 865.28(m), 748.59(w).

3: Add 0.05 mmol (about 30 mg) ligand H_4L^3 , 0.4 mmol $Dy(NO_3)_3 \cdot 6H_2O$ (about 183 mg), 1.5 mL CH_3OH , 0.5 mL CH_3CN and 0.15 mL triethylamine to the Pyrex whose one end is about 25 cm long. In the tube, shake and sonicate for 15 min. Place the sealed Pyrex tube in an oven at 80 °C, take it out three days later, slowly cool to room temperature, and precipitate yellow lumpy crystals. The yield is about 51.3% (calculated with the amount of ligand). Elementary analysis theoretical value ($C_{85}H_{109}Dy_5N_{16}O_{26}$): C, 39.52%; H, 4.25%; N, 8.68%; experimental value: C, 39.35%; H, 4.03%; N, 8.53%. Infrared spectrum data (IR, KBr pellet, cm^{-1}): 3432.18(s), 2374.23(w), 1616.26(vs), 1501.41(s), 1432.50(s), 1379.27(m), 1211.08(m), 866.18(m), 749.33(w).

- [2] Z.-R. Luo, H.-L. Wang, Z.-H. Zhu, T. Liu, X.-F. Ma, H.-F. Wang, H.-H. Zou and F.-P. Liang, Assembly of Dy_{60} and Dy_{30} Cage-Shaped Nanoclusters. *Commun. Chem.* 2020, **3(1)**, 30. <https://doi.org/10.1038/s42004-020-0276-3>.

Table S1. Crystallographic data of the clusters **1–3**.

	1	2	3
Formula	C ₈₄ H ₉₃ Dy ₁₆ N ₂₉ O ₈₀	C ₁₂₇ H ₁₃₄ Dy ₁₀ N ₃₀ O ₅₃	C ₈₅ H ₁₀₉ Dy ₅ N ₁₆ O ₂₆
Formula weight	5388.87	4553.63	2585.39
<i>T</i> , K	100.00(10)	100.00(10)	100.00(10)
Crystal system	monoclinic	triclinic	monoclinic
Space group	<i>P</i> 2 ₁ / <i>n</i>	<i>P</i> -1	<i>I</i> 2/ <i>a</i>
<i>a</i> , Å	22.7736(8)	14.9384(7)	20.1938(3)
<i>b</i> , Å	34.9804(5)	16.6305(6)	23.6957(3)
<i>c</i> , Å	24.2097(10)	17.5360(7)	20.2544(3)
α , °	90	79.223(3)	90
β , °	109.462(4)	88.320(4)	101.8860(10)
γ , °	90	73.352(4)	90
<i>V</i> , Å ³	18184.2(11)	4098.9(3)	9484.1(2)
<i>Z</i>	4	1	4
<i>D</i> _c , g cm ⁻³	1.968	1.844	1.811
μ , mm ⁻¹	6.568	4.583	3.973
<i>F</i> (000)	9984.0	2188.0	5084.0
2θ range for data collection/°	3.224, 60.708	3.748, 49.998	4.11, 60.454
Tot. Data	171635	44675	50510
Uniq. Data	42726	14423	11525
<i>R</i> _{int}	0.0797	0.0561	0.0840
Observed data [<i>I</i> > 2σ(<i>I</i>)]	42726	14423	11525
N _{ref} , N _{par}	709, 1739	99, 1051	2,605
<i>R</i> ₁ ^a (<i>I</i> > 2σ(<i>I</i>))	0.0976	0.0678	0.1363
w <i>R</i> ₂ ^b (all data)	0.3245	0.2110	0.3251
GOF	1.024	1.040	1.257

^a*R*₁ = Σ||F_o| - |F_c|| / Σ|F_o|, ^bw*R*₂ = [Σw(F_o² - F_c²)² / Σw(F_o²)²]^{1/2}

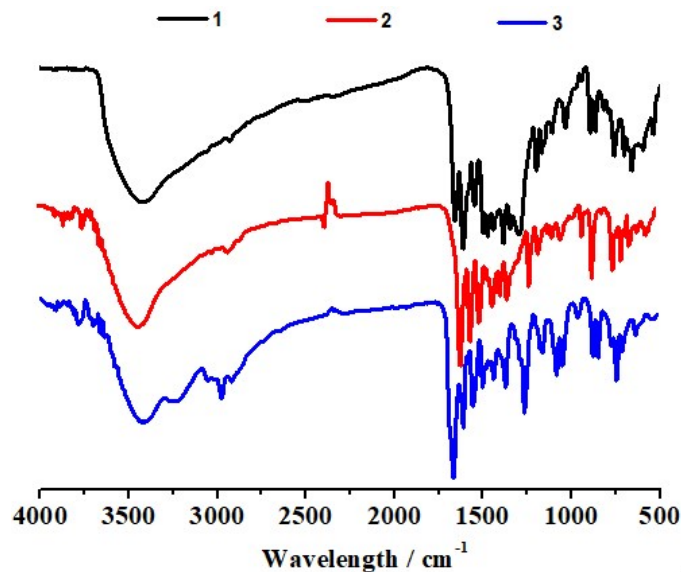


Figure S1. Infrared spectra (IR) of clusters **1–3**.

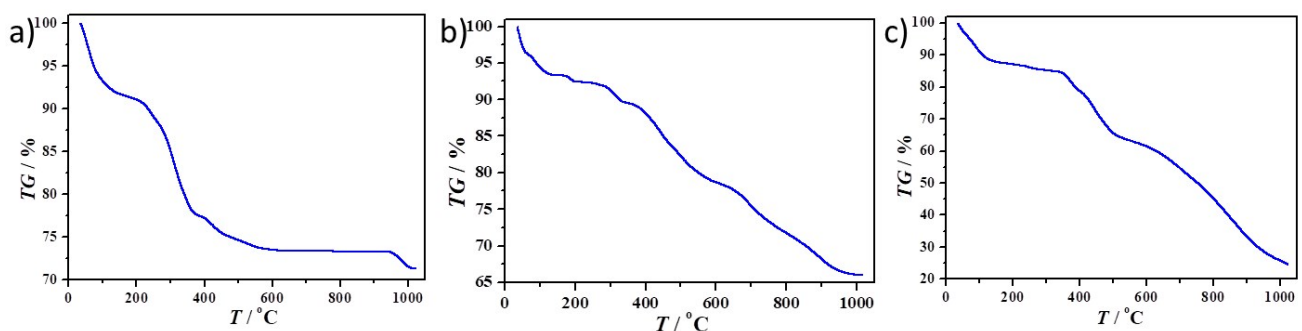


Figure S2. TG curve of clusters **1–3**.

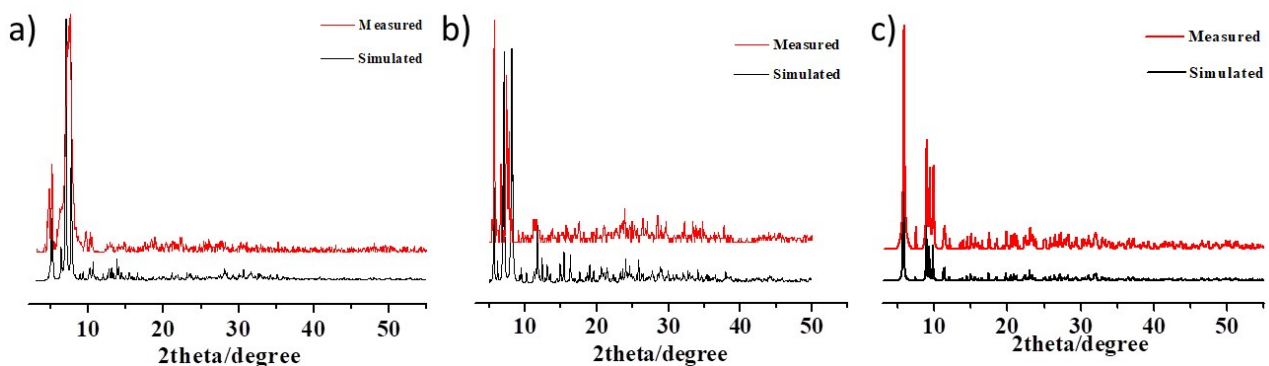


Figure S3. Powder diffraction pattern (PXRD) of clusters **1–3**.

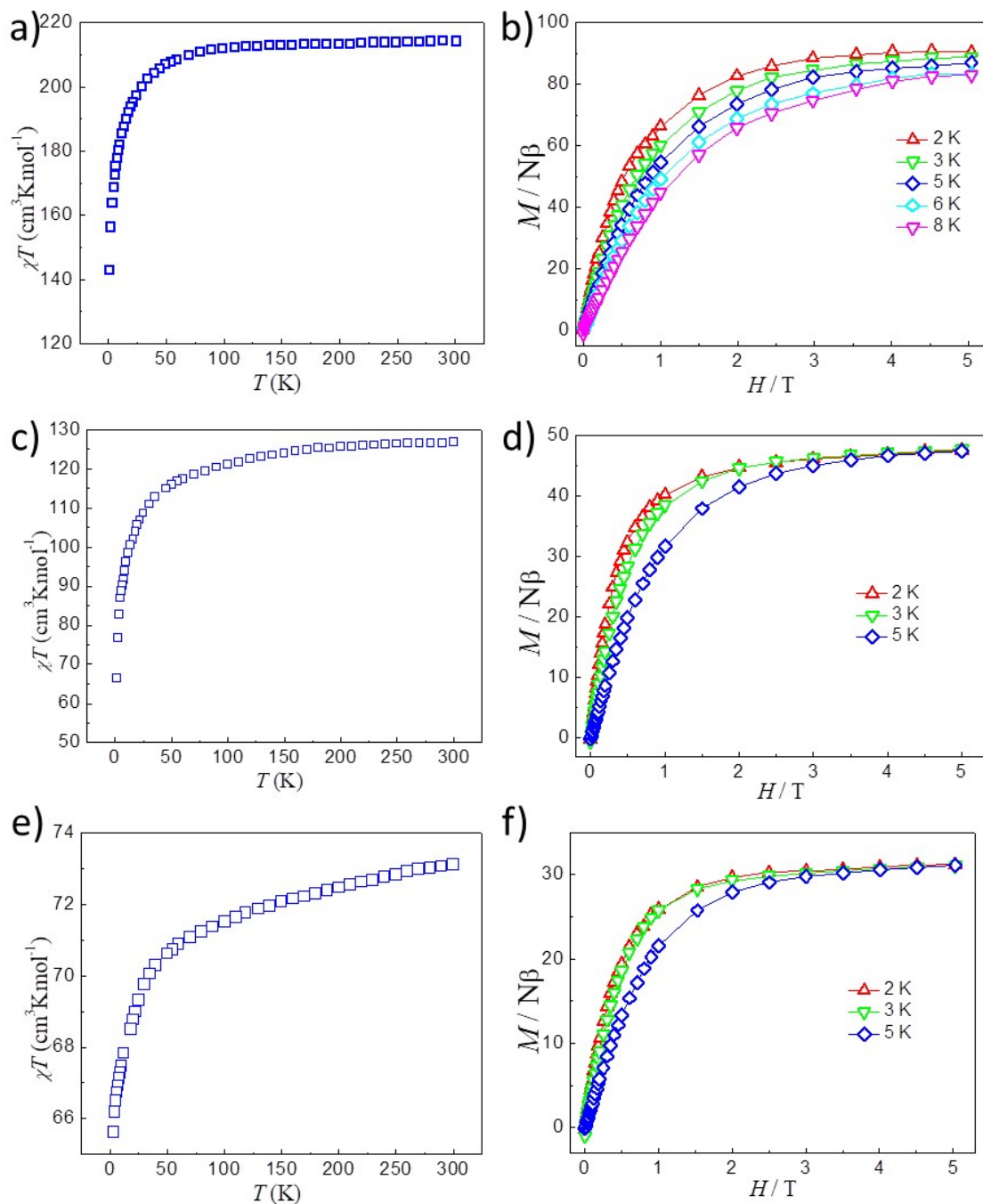


Figure S4. (a, c and e) Temperature dependence of $\chi_m T$ for clusters **1–3**; (b, d and f) M vs. H plots of clusters **1–3**.

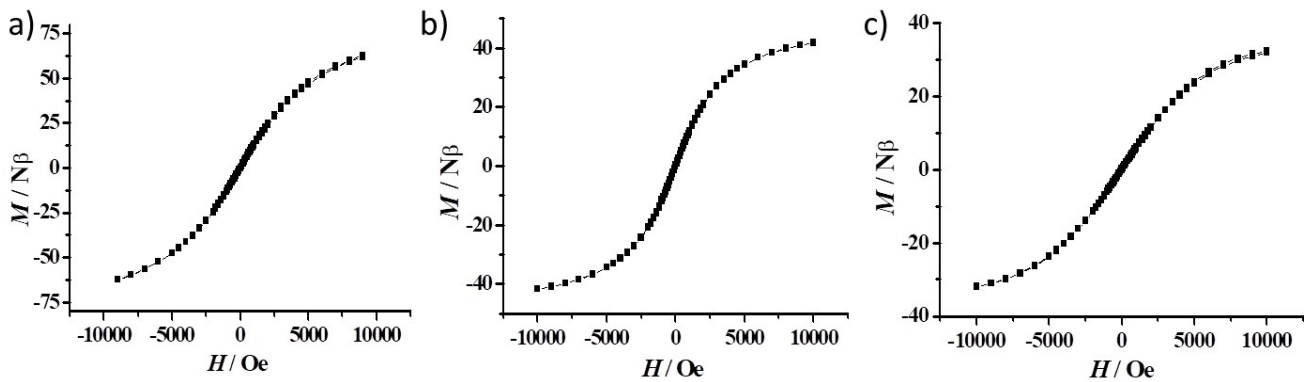


Figure 5. Loop curve graph of clusters **1–3** (a–c) at 2 K.

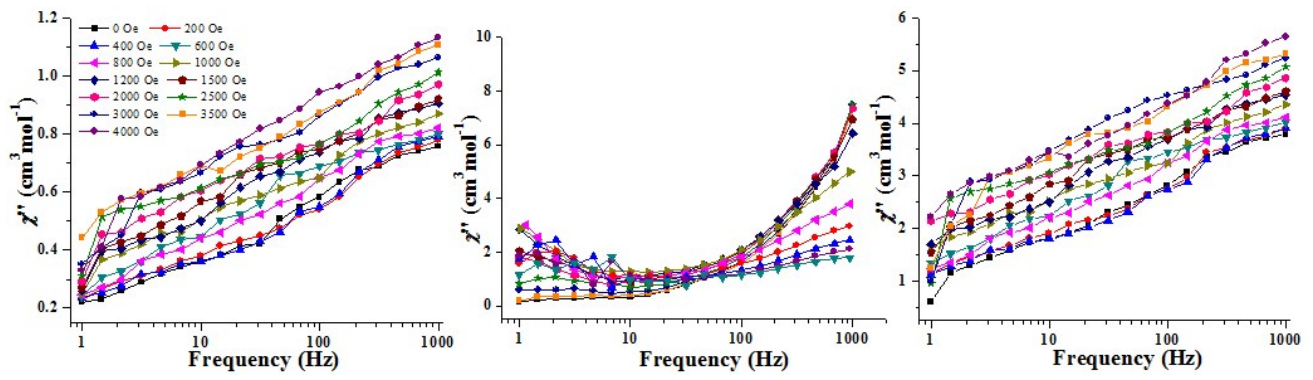


Figure S6. The imaginary parts of the AC susceptibility of clusters **1–3** tested under external DC field values in the range of 0–4000 Oe at 2 K for **1** (left), **2** (middle), and **3** (right).

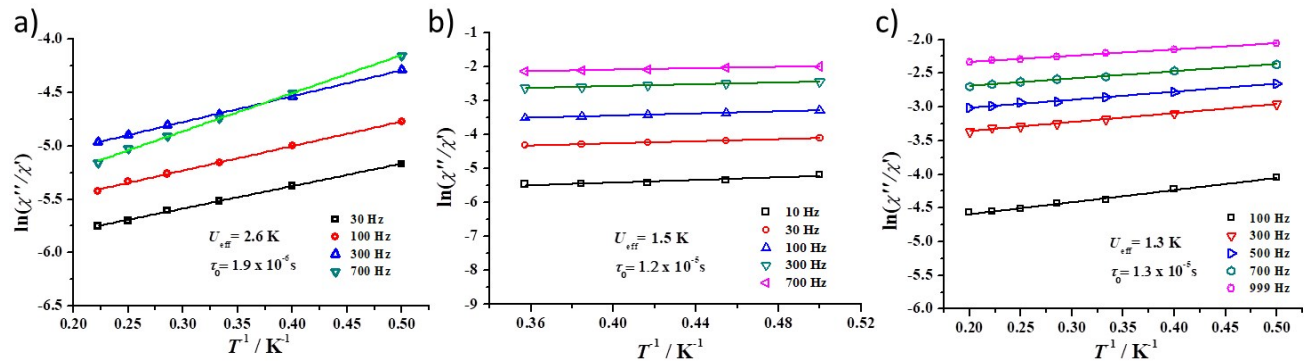


Figure S7. $\ln(\tau)$ vs. T^{-1} plots for **1** (a), **2** (b), and **3** (c), the solid lines show the best fits with the Debye formula (linear).

Table S2. Selected bond lengths (\AA) and angles ($^\circ$) of **1**.

Bond lengths (\AA)					
Dy1-O9	2.344(15)	Dy6-O25	2.411(15)	Dy11-O65	2.660(18)
Dy1-O10	2.357(14)	Dy6-O30	2.36(2)	Dy11-O66	2.45(2)

Dy1-O23	2.363(13)	Dy6-O33	2.391(11)	Dy11-N6	2.486(18)
Dy1-O24	2.358(14)	Dy6-O34	2.375(13)	Dy11-N25	2.862(15)
Dy1-O44	2.46(2)	Dy6-O80	2.351(12)	Dy12-O4	2.393(14)
Dy1-O60	2.514(19)	Dy6-O81	2.395(13)	Dy12-O5	2.363(14)
Dy1-O61	2.49(2)	Dy7-O19	1.939(17)	Dy12-O17	2.315(13)
Dy1-N15	2.482(18)	Dy7-O20	2.897(17)	Dy12-O18	2.416(15)
Dy1-N16	2.491(16)	Dy7-O25	2.81(2)	Dy12-O19	2.419(14)
Dy1-N27	2.93(2)	Dy7-O26	2.038(15)	Dy12-O27	2.359(14)
Dy2-O10	2.376(15)	Dy7-O27	2.68(2)	Dy12-O28	2.345(15)
Dy2-O11	2.319(19)	Dy7-O30	1.960(15)	Dy12-O29	2.416(11)
Dy2-O21	2.289(16)	Dy7-O39	2.60(6)	Dy13-O27	2.290(14)
Dy2-O22	2.310(18)	Dy8-O13	2.386(15)	Dy13-O28	2.416(13)
Dy2-O23	2.442(13)	Dy8-O14	2.475(17)	Dy13-O29	2.389(11)
Dy2-O45	2.391(19)	Dy8-O15	2.466(14)	Dy13-O30	2.269(15)
Dy2-O57	2.26(3)	Dy8-O16	2.353(14)	Dy13-O31	2.298(14)
Dy2-O58	2.64(3)	Dy8-O17	2.709(15)	Dy13-O32	2.338(13)
Dy2-N18	2.47(2)	Dy8-O18	2.343(12)	Dy13-O33	2.395(12)
Dy2-N24	2.671(19)	Dy8-O19	2.370(16)	Dy13-O34	2.385(13)
Dy3-O11	2.558(17)	Dy8-O20	2.333(19)	Dy14-O7	2.389(13)
Dy3-O15	2.404(17)	Dy8-O46	2.54(2)	Dy14-O8	2.329(13)
Dy3-O20	2.421(15)	Dy9-O1	2.215(15)	Dy14-O32	2.424(13)
Dy3-O21	2.19(2)	Dy9-O2	2.341(14)	Dy14-O33	2.387(14)
Dy3-O22	2.567(15)	Dy9-O1	2.215(15)	Dy14-O34	2.369(11)
Dy3-O26	2.337(14)	Dy9-O2	2.341(14)	Dy14-O42	2.46(3)
Dy3-O36	2.32(3)	Dy9-O13	2.362(12)	Dy14-O77	2.53(2)
Dy3-O37	2.329(18)	Dy9-O14	2.32(2)	Dy14-O79	2.43(2)
Dy4-O22	2.315(12)	Dy9-O15	2.370(16)	Dy14-N12	2.486(17)
Dy4-O23	2.287(15)	Dy9-O47	2.37(2)	Dy14-N28	2.77(3)
Dy4-O24	2.348(14)	Dy9-O49	2.42(2)	Dy15-O6	2.310(14)
Dy4-O25	2.297(16)	Dy10-O2	2.349(14)	Dy15-O7	2.320(14)

Dy4-O26	2.332(15)	Dy10-O3	2.365(13)	Dy15-O31	2.351(13)
Dy4-O38	2.79(3)	Dy10-O13	2.400(13)	Dy15-O32	2.349(15)
Dy4-O80	2.568(13)	Dy10-O16	2.360(16)	Dy15-O71	2.37(2)
Dy4-O81	2.312(12)	Dy10-O50	2.56(2)	Dy15-O75	2.56(2)
Dy5-O9	2.366(16)	Dy10-O51	2.47(2)	Dy15-O76	2.44(2)
Dy5-O12	2.318(11)	Dy10-O53	2.516(16)	Dy15-N9	2.476(14)
Dy5-O24	2.408(11)	Dy10-O54	2.401(17)	Dy15-N10	2.469(16)
Dy5-O43	2.414(15)	Dy10-O2	2.349(14)	Dy16-O6	2.378(13)
Dy5-O62	2.555(19)	Dy10-O3	2.365(13)	Dy16-O28	2.391(12)
Dy5-O63	2.46(2)	Dy11-O3	2.342(15)	Dy16-O29	2.369(14)
Dy5-O80	2.335(16)	Dy11-O4	2.325(12)	Dy16-O31	2.384(13)
Dy5-O9	2.366(16)	Dy11-O16	2.395(14)	Dy16-O41	2.40(3)
Dy5-O12	2.318(11)	Dy11-O17	2.304(15)	Dy16-O68	2.48(2)
Dy6-O8	2.386(14)	Dy11-O18	2.385(12)	Dy16-O70	2.46(2)
Dy6-O12	2.395(14)	Dy11-O35	2.423(14)	Dy16-N7	2.482(15)

Bond angles (°)					
O9-Dy1-O10	165.1(6)	O12-Dy6-Dy4	99.8(3)	O4-Dy11-O16	144.5(5)
O9-Dy1-O23	107.2(5)	O12-Dy6-Dy5	40.6(3)	O4-Dy11-O18	71.6(4)
O9-Dy1-O24	67.1(5)	O12-Dy6-Dy13	125.7(3)	O27-Dy12-O4	111.7(6)
O9-Dy1-O44	86.0(6)	O12-Dy6-Dy4	99.8(3)	O27-Dy12-O5	139.4(5)
O9-Dy1-O60	113.2(6)	O19-Dy7-O20	68.3(7)	O27-Dy12-O18	73.5(5)
O9-Dy1-O61	66.0(7)	O19-Dy7-O25	140.1(7)	O27-Dy12-O19	70.9(7)
O9-Dy1-N15	63.7(5)	O19-Dy7-O26	115.4(6)	O27-Dy12-O29	72.8(5)
O9-Dy1-N16	124.9(6)	O19-Dy7-O27	71.6(6)	O28-Dy12-O4	144.2(4)
O10-Dy2-O23	66.4(4)	O19-Dy7-O30	129.4(6)	O28-Dy12-O5	70.9(5)
O10-Dy2-O45	124.4(6)	O19-Dy7-O39	92.8(15)	O30-Dy13-O34	73.8(7)
O10-Dy2-O58	108.5(7)	O26-Dy7-O20	67.6(6)	O30-Dy13-O27	75.6(6)
O10-Dy2-N18	61.9(6)	O26-Dy7-O25	68.0(6)	O30-Dy13-O28	77.2(6)
O10-Dy2-N24	90.0(6)	O16-Dy8-O13	72.2(5)	O30-Dy13-O29	133.3(5)
O11-Dy2-Dy3	46.0(4)	O16-Dy8-O14	75.3(6)	O30-Dy13-O31	115.4(6)

O11-Dy2-O10	124.2(7)	O16-Dy8-O15	131.5(5)	O30-Dy13-O32	144.9(6)
O11-Dy3-O22	62.5(5)	O16-Dy8-O17	67.6(5)	O30-Dy13-O33	75.2(5)
O15-Dy3-Dy2	172.9(3)	O16-Dy8-O19	134.0(6)	O8-Dy14-O7	125.9(5)
O15-Dy3-Dy4	123.5(4)	O16-Dy8-O46	73.1(7)	O8-Dy14-O32	141.6(5)
O15-Dy3-Dy7	70.1(4)	O18-Dy8-O13	128.2(4)	O8-Dy14-O33	74.7(5)
O15-Dy3-Dy7A	83.3(3)	O18-Dy8-O14	139.1(6)	O8-Dy14-O34	71.7(4)
O15-Dy3-O11	132.7(5)	O1-Dy9-O2	137.3(5)	O8-Dy14-O42	103.4(10)
O15-Dy3-O20	68.3(6)	O1-Dy9-O13	153.8(5)	O8-Dy14-O77	77.0(6)
O22-Dy4-O24	90.0(5)	O1-Dy9-O14	110.9(7)	O8-Dy14-O79	131.7(6)
O22-Dy4-O26	74.3(5)	O1-Dy9-O15	83.8(5)	O8-Dy14-N12	73.3(5)
O22-Dy4-O38	72.3(7)	O1-Dy9-O47	84.1(8)	O32-Dy15-O31	76.5(5)
O22-Dy4-O80	148.1(5)	O1-Dy9-O49	89.6(8)	O32-Dy15-O71	141.1(6)
O23-Dy4-O22	75.7(5)	O1-Dy9-N1	72.6(6)	O32-Dy15-O75	68.1(6)
O23-Dy4-O24	74.0(5)	O1-Dy9-N19	87.3(9)	O32-Dy15-O76	74.0(6)
O23-Dy4-O25	98.2(7)	O2-Dy10-O13	67.8(4)	O32-Dy15-N9	141.3(5)
O9-Dy5-O63	147.7(6)	O2-Dy10-O16	102.8(6)	O71-Dy15-O75	145.8(7)
O9-Dy5-O81	130.0(5)	O2-Dy10-O50	118.7(8)	O71-Dy15-O76	138.6(8)
O9-Dy5-N13	63.6(5)	O2-Dy10-O51	78.2(7)	O71-Dy15-N9	77.2(6)
O12-Dy5-Dy1	137.2(5)	O2-Dy10-O53	64.1(6)	O6-Dy16-O28	128.3(5)
O12-Dy5-Dy4	102.2(3)	O2-Dy10-O54	109.4(6)	O6-Dy16-O31	65.8(5)
O12-Dy5-Dy6	42.3(3)	O2-Dy10-N3	63.2(5)	O6-Dy16-O41	126.1(10)
O12-Dy5-O9	123.3(6)	O3-Dy11-O16	68.3(5)	O6-Dy16-O68	114.4(6)
O8-Dy6-O12	82.5(5)	O3-Dy11-O18	130.4(5)	O6-Dy16-O70	70.3(7)
O8-Dy6-O25	118.5(7)	O3-Dy11-O35	75.3(7)	O6-Dy16-N7	62.2(5)
O8-Dy6-O33	73.6(4)	O3-Dy11-O65	125.0(6)	O6-Dy16-N21	89.2(7)
O8-Dy6-O81	146.8(4)	O3-Dy11-O66	148.6(6)	O28-Dy16-O41	72.0(7)

Table S3. Selected bond lengths (\AA) and angles ($^\circ$) of **2**.

Bond lengths (\AA)					
Dy1-O6 ¹	2.348(10)	Dy2-N2	2.552(9)	Dy4-O15	2.431(14)
Dy1-O3	2.304(10)	Dy2-N15	2.519(18)	Dy4-O16	2.596(16)

Dy1-O1	2.350(8)	Dy3-O6	2.274(10)	Dy4-N9	2.563(12)
Dy1-O2	2.352(9)	Dy3-O2 ¹	2.411(10)	Dy4-N8	2.536(11)
Dy1-O22	2.327(9)	Dy3-O7	2.315(9)	Dy5-O3 ¹	2.318(10)
Dy1-O21 ¹	2.337(10)	Dy3-O19	2.326(11)	Dy5-O1 ¹	2.420(10)
Dy1-N1	2.510(11)	Dy3-O20	2.345(11)	Dy5-O8	2.334(10)
Dy1-N4 ¹	2.521(11)	Dy3-O13	2.168(11)	Dy5-O14	2.377(10)
Dy2-O4 ¹	2.279(9)	Dy3-N11	2.446(12)	Dy5-O12	2.197(11)
Dy2-O4	2.257(13)	Dy4-O1 ¹	2.393(9)	Dy5-O9	2.442(12)
Dy2-O5	2.359(15)	Dy4-O2 ¹	2.421(8)	Dy5-O10	2.493(15)
Dy2-N13	2.542(11)	Dy4-O8	2.355(10)	Dy5-N6	2.443(12)
Dy2-N3	2.534(9)	Dy4-O7	2.389(11)	Dy5-N5	2.869(16)
Dy2-N14	2.521(11)	Dy4-O18	2.388(13)		
Bond angles (°)					
O6 ¹ -Dy1-O1	92.4(3)	O4 ¹ -Dy2-N3	85.0(3)	O7-Dy4-O1 ¹	105.9(3)
O6 ¹ -Dy1-O2	72.9(3)	O4 ¹ -Dy2-N14	139.0(4)	O7-Dy4-O2 ¹	67.4(3)
O6 ¹ -Dy1-N1	127.0(3)	O4-Dy2-N14	84.3(4)	O7-Dy4-O15	103.2(5)
O6 ¹ -Dy1-N4 ¹	70.4(3)	O4 ¹ -Dy2-N2	85.0(3)	O7-Dy4-O16	62.1(5)
O3-Dy1-O6 ¹	161.0(3)	O6-Dy3-O2 ¹	73.1(3)	O7-Dy4-N9	62.4(4)
O3-Dy1-O1	71.9(3)	O6-Dy3-O7	97.4(4)	O7-Dy4-N8	125.0(4)
O3-Dy1-O2	91.9(3)	O6-Dy3-O19	166.7(4)	O18-Dy4-O1 ¹	130.2(4)
O6 ¹ -Dy1-O1	92.4(3)	O6-Dy3-O20	92.0(4)	O3 ¹ -Dy5-O1 ¹	70.5(3)
O3-Dy1-O22	108.6(4)	O6-Dy3-N11	112.4(4)	O3 ¹ -Dy5-O8	87.8(3)
O4-Dy2-O5	152.7(4)	O2 ¹ -Dy3-N11	132.7(4)	O3 ¹ -Dy5-O14	92.1(3)
O4 ¹ -Dy2-N13	139.1(4)	O7-Dy3-O2 ¹	68.7(3)	O3 ¹ -Dy5-O9	151.1(5)
O4-Dy2-N13	84.6(4)	O7-Dy3-O19	84.2(4)	O3 ¹ -Dy5-O10	152.9(4)
O4-Dy2-N3	91.4(4)	O7-Dy4-O1 ¹	105.9(3)	O3 ¹ -Dy5-N6	106.5(4)

Table S4. Selected bond lengths (Å) and angles (°) of **3**.

Bond lengths (Å)			
Dy1-O2 ¹	2.357(15)	Dy2-N3	2.493(18)
Dy1-O2	2.357(15)	Dy2-O6	2.221(15)

Dy1-O1	2.147(15)	Dy3-O5	2.369(12)
Dy1-O1 ¹	2.147(15)	Dy3-O4	2.191(16)
Dy1-O7 ¹	2.613(16)	Dy3-O3	2.354(14)
Dy1-O7	2.613(15)	Dy3-O11 ¹	2.413(15)
Dy1-N1	2.481(19)	Dy3-N6	2.511(18)
Dy1-N1 ¹	2.481(18)	Dy3-O6 ¹	2.271(16)
Dy2-O5	2.286(7)	Dy3-O10	2.198(14)
Dy2-O2	2.327(15)	Dy2-O9 ¹	2.478(17)
Dy2-O3	2.328(15)	Dy2-N4	2.507(17)
Dy2-O7 ¹	2.516(14)		

Bond angles (°)			
O2-Dy1-O2 ¹	112.3(7)	O5-Dy2-N3	149.2(4)
O2 ¹ -Dy1-O7	66.1(5)	O2-Dy2-O3	161.3(5)
O2-Dy1-O7 ¹	66.1(5)	O2-Dy2-O7 ¹	68.1(5)
O2-Dy1-O7	70.6(5)	O5-Dy3-O11 ¹	95.8(5)
O2 ¹ -Dy1-O7 ¹	70.6(5)	O5-Dy3-N6	131.1(4)
O2-Dy1-N1	64.5(6)	O4-Dy3-O5	154.6(4)
O2 ¹ -Dy1-N1	145.2(6)	O4-Dy3-O3	130.8(5)
O2 ¹ -Dy1-N1 ¹	64.5(6)	O4-Dy3-O11 ¹	93.7(6)
O5-Dy2-O2	99.0(6)	O4-Dy3-N6	70.5(6)
O5-Dy2-O3	76.5(5)	O4-Dy3-O6 ¹	85.5(6)
O5-Dy2-O7 ¹	82.6(5)	O4-Dy3-O10	98.8(7)
O5-Dy2-O9 ¹	129.1(4)	O3-Dy3-O5	74.4(4)
O5-Dy2-N4	131.0(6)	O3-Dy3-O11 ¹	76.6(5)